Forest Service
U.S. DEPARTMENT OF AGRICULTURE
Geospatial Technology and Applications Center
October 6, 2023

US Forest Service Landscape Change Monitoring System Methods

Version: 2022.8

Mapping Areas: Conterminous United States, Southeastern Alaska, Puerto Rico – U.S. Virgin Islands, and Hawaii

Geospatial Technology and Applications Center (GTAC)

125 S. State Street, Suite 7105, Salt Lake City, Utah 84138
apps.fs.usda.gov/gtac/

Ian Housman
Technical Lead
Senior Remote Sensing Specialist
RedCastle Resources, onsite contractor
801-975-3366, ian.housman@usda.gov

Josh Heyer
Production Lead
Geospatial Specialist
RedCastle Resources, onsite contractor
joshua.heyer@usda.gov

Elizabeth Hardwick
Production Lead
Remote Sensing Specialist
RedCastle Resources, onsite contractor
elizabeth.hardwick@usda.gov

Jennifer Lecker
Geospatial Project Manager
RedCastle Resources, onsite contractor
801-975-3427, jennifer.lecker@usda.gov

Kevin Megown
Program Leader
Resource Mapping, Inventory, and Monitoring (RMIM)
801-975-3750, kevin.megown@usda.gov

Jennifer Ross
Geospatial Specialist
Resource Mapping, Inventory, and Monitoring (RMIM)
517-884-8053, jennifer.ross@usda.gov

Nathan Pugh
Geospatial Specialist
TDIM Program Lead
801-975-3827, nathan.pugh@usda.gov

USDA Non-Discrimination Statement

In accordance with Federal civil rights law and U.S. Department of Agriculture (USDA) civil rights regulations and policies, the USDA, its Agencies, offices, and employees, and institutions participating in or administering USDA programs are prohibited from discriminating based on race, color, national origin, religion, sex, gender identity (including gender expression), sexual orientation, disability, age, marital status, family/parental status, income derived from a public assistance program, political beliefs, or reprisal or retaliation for prior civil rights activity, in any program or activity conducted or funded by USDA (not all bases apply to all programs). Remedies and complaint filing deadlines vary by program or incident.

Persons with disabilities who require alternative means of communication for program information (e.g., Braille, large print, audiotape, American Sign Language, etc.) should contact the responsible Agency or USDA's TARGET Center at (202) 720-2600 (voice and TTY) or contact USDA through the Federal Relay Service at (800) 877-8339. Additionally, program information may be made available in languages other than English.

To file a program discrimination complaint, complete the USDA Program Discrimination Complaint Form, AD-3027, found online at How to File a Program Discrimination Complaint and at any USDA office or write a letter addressed to USDA and provide in the letter all of the information requested in the form. To request a copy of the complaint form, call (866) 632-9992. Submit your completed form or letter to USDA by: (1) mail: U.S. Department of Agriculture, Office of the Assistant Secretary for Civil Rights, 1400 Independence Avenue, SW, Washington, D.C. 20250-9410; (2) fax: (202) 690-7442; or (3) email: program.intake@usda.gov.

USDA is an equal opportunity provider, employer, and lender.

Housman, I.W.; Heyer, J.P.; Hardwick, E.; Lecker, J.; Megown, K.; Ross, J.; Pugh, N. 2023. US Forest Service Landscape Change Monitoring System Methods Version 2022.8. GTAC-10252-RPT3. Salt Lake City, UT: U.S. Department of Agriculture, Forest Service, Geospatial Technology and Applications Center. 27 p.

Contents

LCMS Conterminous United States, Southeastern Alaska, Puerto Rico – U.S. Virgin Islands, and Hawaii Version 2022.8 Release Notes

Any changes to the methods from LCMS version 2021.7 outlined below in this document will be reflected in this list

- Computing platforms
  - No changes

- Model calibration data
  - No changes

- Model predictor data
  - The United States Geologic Survey (USGS) Landsat collection 2 data were used in generating annual composites.
  - In addition to Landsat 4, 5, 7, and 8, Landsat 9 is now included as well.
  - LandTrendr and CCDC predictor data were updated with data generated from Landsat collection 2 data.
  - Surface Reflectance data was used to run CCDC for the CONUS.
  - CCDC NBR, NDMI and wetness predictors were not included.
  - No Landsat thermal data were included as predictor variables in CONUS, SEAK, PRUSVI or HA.
  - Use the USGS 3D Elevation Program (3DEP) data for our terrain predictors.

- Modeling (Supervised Classifications)
  - No changes

- LCMS products
  - Production of Hawaii LCMS is ongoing, and the data release is upcoming.
  - For PRUSVI, low developed probabilities were excluded to limit the commission of developed in non-developed classes. Through qualitative assessment of the land use assembled maps we used the 70th percentile developed raw probabilities in highest probability classification, which excluded low developed probabilities and allowed other land use class probabilities to be considered instead in classification. Excluding low developed probabilities helped limit developed commission in uncertain land use types such as agriculture and rangelands.

LCMS Conterminous United States and Southeastern Alaska Version 2021.7 Release Notes

Any changes to the methods from LCMS version 2020.5 outlined below in this document will be reflected in this list

- Computing platforms
  - No changes

- Model calibration data
  - Additional training locations were collected over areas of lava rock in the Southwestern US and coastal wetlands in Southern Texas to help the models avoid classifying these areas as developed.

- Model predictor data
    - In order to avoid masking out areas of water that were not present for the majority of the analysis period, for dark pixels only (Sum of NIR and SWIR1 bands <= 0.175), the Temporal Dark Outlier Mask (TDOM) method now utilizes a shorter 3-year time window (One year plus and minus the year of the composite – e.g. for a year 2000 composite, the years 1999-2001 would be included in the TDOM statistics) to derive statistics to identify outliers. All other pixels continue to use the statistics from 1985-2020. This helps avoid masking areas of water that were not present for most of the analysis period.
    - Landsat/Sentinel 2 composites were not used directly as predictor variables.
    - Interpolated values from both LandTrendr and CCDC were included as predictor variables to allow for more complete maps (These areas can be removed by using the QA band described below).
    - Landsat thermal data were included as predictor variables in CONUS, but not SEAK.

- Modeling (Supervised Classifications)
    - No changes

- LCMS products
    - Since change is intended to depict vegetation cover change, change is excluded from any pixel classified water, snow/ice, or barren for all years.
    - Ancillary information on the origin of the annual LCMS product output values are now provided as part of a QA bit layer. This layer includes whether an interpolated value was used to produce the LCMS output, the sensor, and the day of year the value came from.
    - A postprocessing rule is now applied to land use maps. Since heavily treed developed areas are frequently erroneously classified as forest land use, we now require that if a pixel has been classified as developed it cannot subsequently change to forest. To avoid inadvertently increasing commission errors in areas that were initially erroneously classified as developed, we limit this ruleset to pixels that are a maximum of two pixels away from a pixel classified as built-up in the Landsat-based Global Human Settlement Layer built-up area grid (GHSL; Corbane et al., 2018) at any of the mapped GHSL years (1975, 1990, 2000, and 2014).

Executive Summary

The Landscape Change Monitoring System (LCMS) is a remote sensing-based system produced by the United States Department of Agriculture, Forest Service (USFS) for mapping and monitoring changes

related to vegetation canopy cover, as well as land cover and land use. Data produced by LCMS extend from 1985 to the most recently completed growing year. LCMS is intended to provide a consistent monitoring method for applications including, but not limited to, post-disturbance monitoring, broad-scale vegetation cover change, land cover and land use conversion trends monitoring, and sensitive habitat monitoring.

This document details the methods employed to create all map products for LCMS version 2022.8. These methods will be revisited annually to ensure they reflect the best available science. Current methods involve utilizing Landsat and Sentinel 2 data in the Landsat-based detection of Trends in Disturbance and Recovery (LandTrendr) and Landsat data in the Continuous Change Detection and Classification (CCDC) temporal segmentation algorithms. Outputs from these algorithms are used as predictor variables in random forest models that are calibrated using training data from TimeSync. The broad categories of LCMS products are vegetation cover change, land cover, and land use.

All LCMS products are freely available for download at the LCMS website.

Users can interactively visualize and summarize the data at the LCMS Viewer.

Background

Our landscape is continually changing. Monitoring change in vegetation cover and conversion of land cover and land use is important for making data-driven land management decisions. The USFS has developed the Landscape Change Monitoring System (LCMS) to consistently monitor changes in vegetation cover, land cover, and land use across the United States from 1985 to present.

The LCMS Science Team initially developed all LCMS methods (Cohen et al., 2018; Healey et al., 2018). This team evaluated the best available science about landscape change detection methods and provided guidance for the adapted operational LCMS methods employed by the LCMS Production Team described in this document.

The Science Team and Production Team jointly re-evaluate the methods annually to ensure the mapping process is still based on the best available science. This document describes the methods used to create LCMS version 2022.8 products. The version naming convention is YYYY.v where “YYYY” denotes the most recent year mapped, and the “v” denotes the version of the methods used. We recreate all map products annually from 1985 to the most recent full growing season. Annual production ensures LCMS methods can be updated when appropriate and all maps will be produced in a consistent manner.

LCMS mapping areas include all the United States and its territories. The current operational set of outputs cover the conterminous United States (CONUS), southeastern Alaska (SEAK), Puerto Rico U.S. Virgin Islands (PRUSVI). Hawaii (HA) production efforts are ongoing, and the HA LCMS data release is upcoming. This document outlines methods used over the study areas.

The core LCMS products are annual vegetation cover change, land cover, and land use raster maps. Vegetation cover change is broken into slow loss, fast loss, and gain. Change products are intended to address needs centered around monitoring variations in vegetation cover or water extent that may or may not result in a transition of land cover and/or land use. Land cover products can be used to meet more general land cover monitoring needs over time. Land use products can be used to monitor land use conversion patterns.

Methods

Computing platforms

LCMS utilizes Google Earth Engine (GEE; Gorelick 2017) through an enterprise agreement between the USFS and Google, for all remote sensing raster data acquisition and processing. GEE is a parallel computing environment that provides access to many publicly available earth observation datasets, along with common data processing methods, and computing infrastructure to process these data. While GEE's data processing methods are quite extensive, currently it cannot meet the breadth of methods available in common scientific computing platforms such as R and the Python package Scikit-Learn (Pedregosa et al., 2011). Due to these limitations, we use Scikit-Learn for sample design, model predictor variable selection, and model validation.

Model calibration data

All supervised statistical models need a set of calibration data (dependent variable or training data), and predictor variables (independent variables) to train the model. The model is then applied to the predictor data where there are no calibration data. This section will outline how LCMS calibration data locations are selected and attributed.

Model calibration data sample design

The goal of a sample design is to efficiently sample the expected variability of the dependent variable. Since LCMS maps vegetation cover change, land cover, and land use, the sample design needs to account for expected variability in each of these categories across the US.

Pilot projects we completed throughout the United States revealed that many of the classes, such as vegetation cover loss and impervious land cover, are relatively rare across the landscape. The simple random sample we initially used proved insufficient to capture an adequate proportion of these rare classes. To improve our sampling approach, we moved to a stratified random sample design following the guidance from Olofsson et al., (2014). Specifically, "*The recommended allocation of sample size to the strata defined by the map classes is to increase the sample size for the rarer classes making the sample size per stratum more equitable than what would result from proportional allocation, but not pushing to the point of equal allocation."*

Based on this guidance, we stratify the landscape using the 2016 National Land Cover Database (NLCD) land cover / land use map for CONUS (Yang et al., 2018), paired with LandTrendr (Kennedy et al., 2010; Kennedy et al., 2018) for SEAK and HA (Figures 1,2, and 4). For PRUSVI, the sample design uses land cover data from Helmer et al. (2002) for stratification (Figure 3).

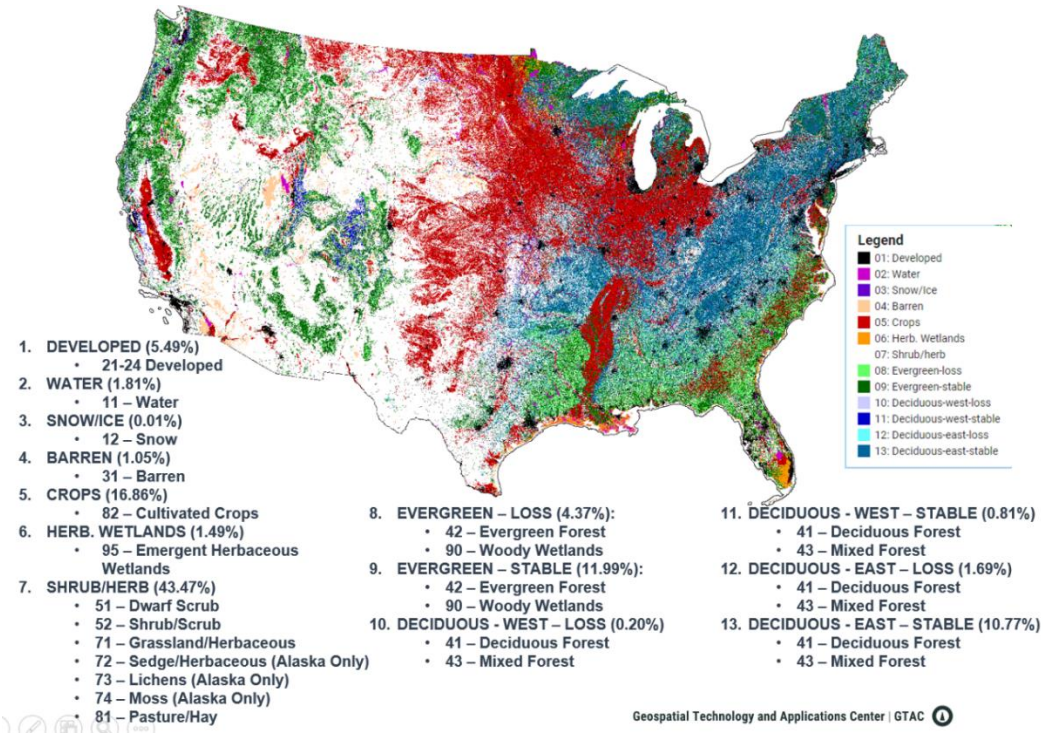

Figure 1. – Map depicting strata used for the Land Change Monitoring System (LCMS) conterminous United States (CONUS) calibration/validation sample design. Final strata are listed below the map, with the percentage of total pixels represented by that stratum in parentheses and National Land Cover Database (NLCD) land cover classes included in that stratum listed below (Yang et al., 2018).

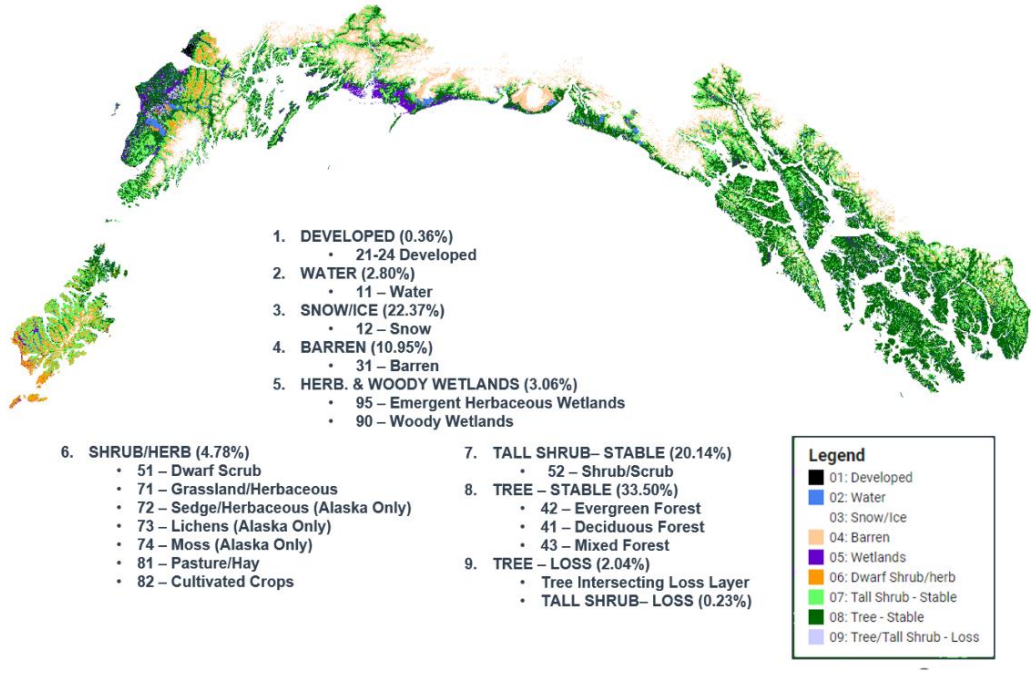

Figure 2. – Map depicting strata used for the Land Change Monitoring System Southeast Alaska (SEAK) calibration/validation sample design. Final strata are listed below the map, with the percentage of total pixels represented by that stratum in parentheses and National Land Cover Dataset (NLCD) land cover classes included in that stratum listed below (Yang et al., 2018).

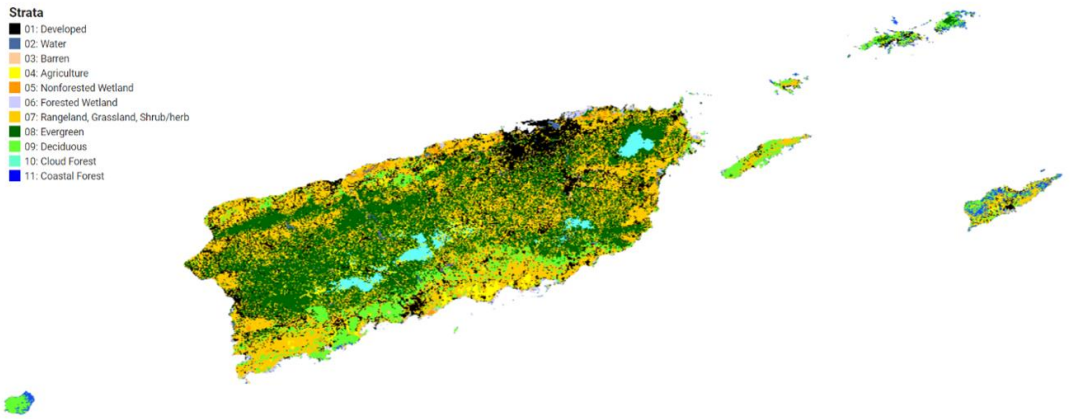

1.	Developed:	14.1%	5.	Non-Forested Wetland:	0.7%	9.	Deciduous:	8.4%
2.	Water:	1.1%	6.	Forested Wetland:	0.9%	10.	Cloud Forest:	2.5%
3.	Barren:	1.0%	7.	Rangeland, Grassland, Shrub & Herb:	34.3%	11.	Coastal Mixed Forest:	1.0%
4.	Agriculture:	3.4%	8.	Evergreen:	32.4%			

Figure 3. – Map depicting strata used for the Land Change Monitoring System Puerto Rico U.S. Virgin Islands (PRUSVI) calibration/validation sample design. Final strata are listed below the map, with the percentage of total pixels represented by that stratum included. PRUSVI uses land cover data from Helmer et al. (2002) for stratification.

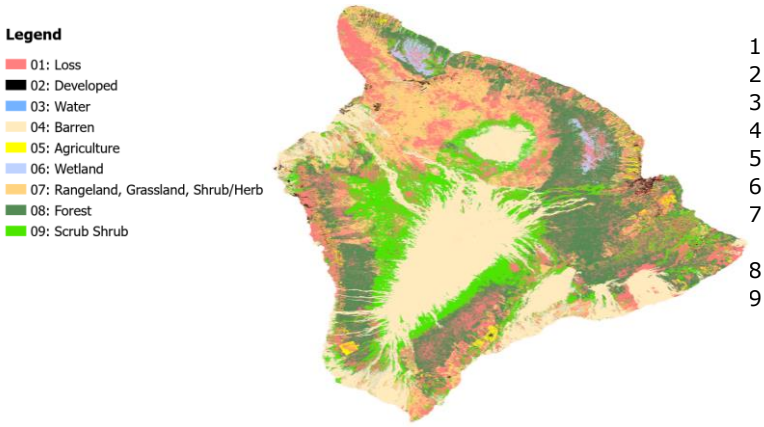

1.	Loss:	19.0%
2.	Developed	0.6%
3.	Water	13.2%
4.	Barren	20.5%
5.	Agriculture	0.9%
6.	Wetland	2.5%
7.	Rangeland, Grassland, Shrub/Herb	12.5%
8.	Forest	18.8%
9.	Scrub Shrub	12.0%

Figure 4. – Map depicting strata used for the Land Change Monitoring System Hawaii (HA) calibration/validation sample design. Final strata are listed next to the map, with the percentage of total pixels represented by that stratum included. HA uses 2011 NLCD land cover from the 2016 NLCD land cover dataset (Yang et al., 2018) for stratification.

We chose the strata shown for CONUS (**Error! Reference source not found.**), SEAK (*Table 1*), PRUSVI (Table 3), and HA (Table 4) to adequately sample rare classes that are of specific interest to LCMS applications and/or had high model error in LCMS pilot studies. This includes tree loss, deciduous tree loss in the western US, wetlands, and developed areas. Areas such as water and snow/ice typically have low model error, and therefore we allocated fewer samples to those classes.

The final sample size was 10,010 across CONUS, 929 across SEAK, 1100 across PRUSVI, and 1000 across HA. We started the final sample count with an allocation halfway between equal and proportional. We set a maximum value of 1000 for CONUS, and 200 for SEAK, PRUSVI, and HA for each stratum. We then proportionally recursively allocated the remainder. Lastly, we set a fixed sample number of 30 for snow/ice and 200 (30 for SEAK) for water (because these are "easier", less variable classes). For PRUSVI, we set a fixed sample number of 30 for water and barren. For HA, we set a fixed sample number of 30 for water. We allocated the remaining samples equally across the three disturbance (*loss*) strata. Tables 1, 2, 3 and 4 the final sample counts by strata for CONUS, SEAK, PRUSVI and HA respectively.

Table 1. – Final sample counts by strata for the CONUS calibration sample.

Stratum	Count	Percent	Proportional	Equal	Equal/ Proportional	Min/ Max	Set Values Applied
01: Developed	472588767	5.5%	548	625	587	977	999
02: Water	148583076	1.7%	173	625	399	521	200
03: Snow/Ice	571498	0.01%	1	625	313	313	30
03: Barren	90344250	1.1%	105	625	365	439	578
04: Agriculture	1458578963	16.9%	1690	625	1158	1055	1007
05: Herb. Wetlands	124067106	1.4%	144	625	385	486	659
06: Shrub/herb	3755611086	43.5%	4350	625	2488	1063	1010
05: Evergreen-loss	377541936	4.8%	438	625	532	841	1280
06: Evergreen-stable	1035526514	12.0%	1200	625	913	1050	988
07: Deciduous-west-loss	17165119	0.2%	20	625	323	336	709
08: Deciduous-west-stable	69803183	0.8%	81	625	353	412	533
09: Deciduous-east-loss	146249349	1.7%	170	625	398	518	984
13: Deciduous-east-stable	931577696	10.8%	1079	625	852	1050	990
14: Volcanic Rocks	1396100	0.02%	2	625	314	315	34
15: S. Texas Coastal Wetlands	1205013	0.01%	2	625	314	315	33
16: S. Texas Oil & Gas	3555467	0.04%	5	625	315	317	33
TOTAL:	8634365129	100%	10008	10000	10009	10008	10067

Table 1. – Final sample counts by strata for the SEAK calibration sample.

Stratum	Count	Percent	Proportional	Equal	Equal/ Proportional	Min/Max	Set Values Applied
01: Developed	670861	0.4%	4	103	54	54	30
02: Water	5165532	2.8%	26	103	65	65	30
03: Snow/Ice	41313696	22.4%	207	103	155	155	30
04: Barren	20211947	10.9%	102	103	103	103	80
05: Herb. & Woody Wetlands	5642129	3.1%	29	103	66	66	79
06: Dwarf Shrub/Herb	8818866	4.8%	45	103	74	74	87

07: Tall Shrub – Stable	37192517	20.1%	187	103	145	145	167
08: Tree – Stable	61864335	33.5%	310	103	207	207	207
09: Tree/Tall Shrub – Loss	3769700	2.0%	19	103	61	61	219
TOTAL:	184649583	100%	929	927	930	930	929

Table 3. – Final sample counts by strata for the PRUSVI calibration sample.

Stratum	Count	Percent	Proportional	Equal	Equal/ Proportional	Min/ Max	Set Values Applied
01: Developed	1450331	14.1%	156	100	128	157	157
02: Water	113212	1.2%	13	100	57	59	30
03: Barren	110101	1.1%	12	100	56	58	30
04: Agriculture	344785	3.4%	37	100	69	76	76
05: Non-Forested Wetland	71185	0.7%	8	100	54	55	76
06: Forested Wetland	92958	0.9%	10	100	55	57	57
07: Rangeland	3519261	34.3%	378	100	239	200	200
08: Evergreen	3325898	32.4%	357	100	229	200	200
09: Deciduous	865643	8.4%	93	100	97	114	114
10: Cloud Forest	258676	2.5%	28	100	64	69	100
11: Coastal Mixed Forest	102288	1.0%	11	100	56	58	60
TOTAL:	1103	100%	1103	1100	1104	1103	1100

Table 4. – Final sample counts by strata for the Hawaii calibration sample.

Stratum	Count	Percent	Proportional	Equal	Equal/ Proportional	Min/ Max	Set Values Applied
01: Developed	77810	0.6%	6	112	152	152	80
02: Water	1756563	13.2%	132	112	59	59	30
03: Barren	2742909	20.5%	206	112	122	122	50
04: Agriculture	121505	0.9%	10	112	159	159	70
05: Wetland	332267	2.5%	25	112	61	61	70
06: Rangeland	1671666	12.5%	126	112	69	69	150
07: Forest	2508101	18.8%	188	112	119	119	230
08: Scrub shrub	1602192	12.0%	120	112	150	150	120
09: Loss	2539975	19.0%	191	112	116	116	200
TOTAL:	13352988	100%	1004	1008	1007	1007	1000

Calibration Data Collection

We collected model calibration data using the TimeSync attribution tool (Cohen et al., 2010). TimeSync is a web-based application that allows users to look at a time series of Landsat images, along with available high-resolution images in Google Earth Pro and other ancillary data in the Ancillary Data Viewer web application, which is made at the Geospatial Technology and Applications Center (GTAC), to attribute yearly land cover, land use, and change process at each training point location (Figure 5).

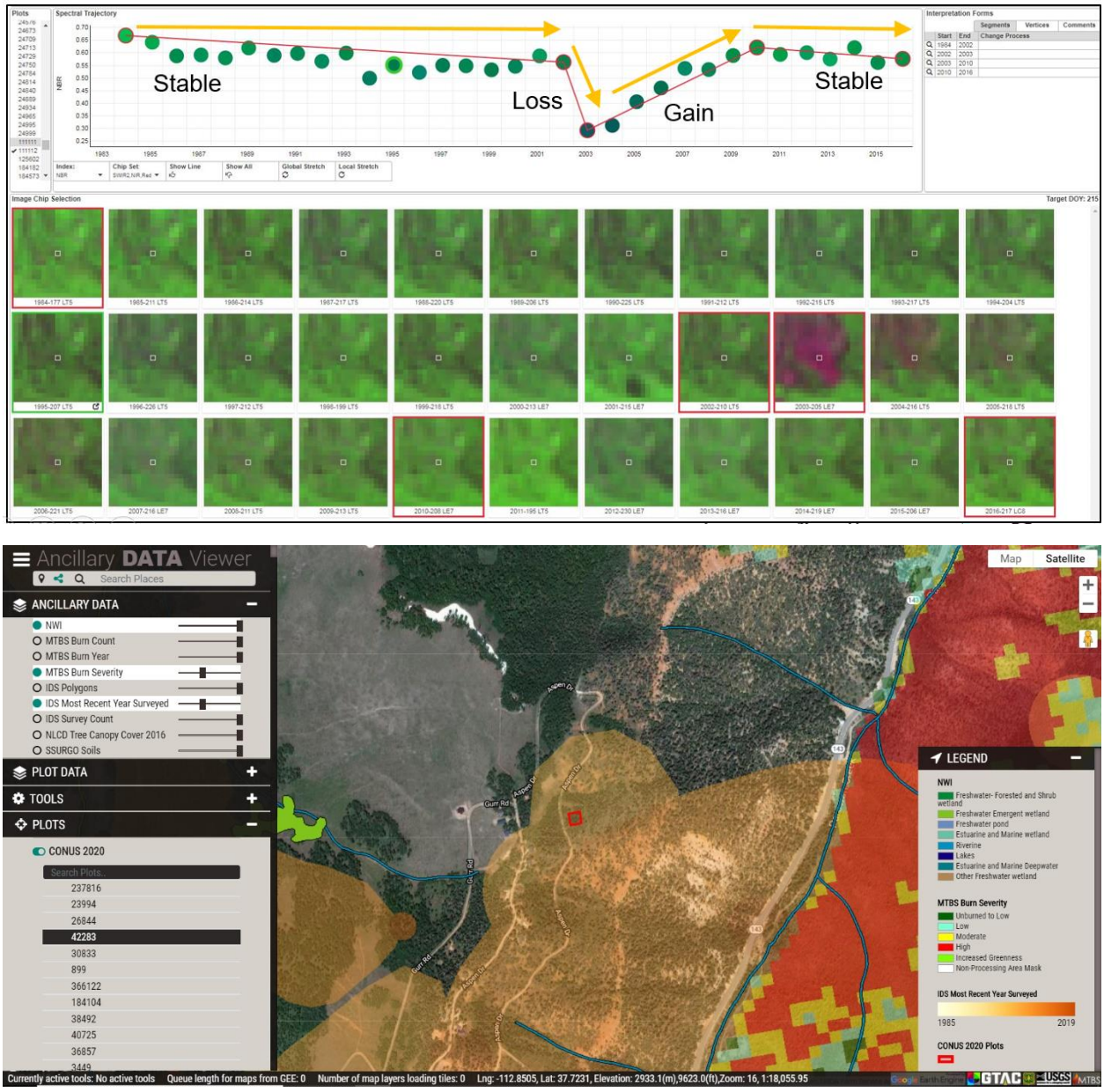

Figure 5. – Example of the TimeSync tool (top) and the Ancillary Data Viewer (bottom). These tools, along with Google Earth Pro, are used in unison to attribute change process, land cover, and land use for each year for each model calibration plot.

LCMS TimeSync interpretation utilizes the Land Change Monitoring, Assessment, and Projection (LCMAP)/LCMS Joint Response Design. This response design provides a consistent method for attributing a common set of classes for change process, land cover, and land use (see supplementary materials in Pengra et al., 2020). The classes and their definitions are as follows:

- Change process
    1. FIRE: Land altered by fire, regardless of the cause of the ignition (natural or anthropogenic), severity, or land use.
    2. HARVEST: Forest land where trees, shrubs or other vegetation have been severed or removed by anthropogenic means. Examples include clearcutting, salvage logging after fire or insect outbreaks, thinning and other forest management prescriptions (e.g., shelterwood/seedtree harvest).
    3. MECHANICAL: Non-forest land where trees, shrubs or other vegetation has been mechanically severed or removed by chaining, scraping, brush sawing, bulldozing, or any other methods of non-forest vegetation removal.
    4. STRUCTURAL DECLINE: Land where trees or other woody vegetation is physically altered by unfavorable growing conditions brought on by non-anthropogenic or non-mechanical factors. This type of loss should generally create a trend in the spectral signal(s) (e.g., NDVI decreasing, Wetness decreasing; SWIR increasing; etc.), however the trend can be subtle. Structural decline occurs in woody vegetation environments, most likely from insects, disease, drought, acid rain, etc. Structural decline can include defoliation events that do not result in mortality such as in Gypsy moth and spruce budworm infestations which may recover within one or two years.
    5. SPECTRAL DECLINE: A plot where the spectral signal shows a trend in one or more of the spectral bands or indices (e.g., NDVI decreasing, Wetness decreasing; SWIR increasing; etc.). Examples include cases where: a) non-forest/non-woody vegetation shows a trend suggestive of decline (e.g. NDVI decreasing, Wetness decreasing; SWIR increasing; etc.); or b) woody vegetation shows a decline trend that is not related to the loss of woody vegetation, such as when mature tree canopies close resulting in increased shadowing, when species composition changes from conifer to hardwood, or when a dry period (as opposed to stronger, more acute drought) causes an apparent decline in vigor, but no loss of woody material or leaf area.
    6. WIND/ICE: Land (regardless of use) where vegetation is altered by wind from hurricanes, tornados, storms, and other severe weather events including freezing rain from ice storms.
    7. HYDROLOGY: Land where flooding has significantly altered woody cover or other land cover elements regardless of land use (e.g., new mixtures of gravel and vegetation in and around streambeds after a flood).
    8. DEBRIS: Land (regardless of use) altered by natural material movement associated with landslides, avalanches, volcanos, debris flows, etc.
    9. OTHER: Land (regardless of use) where the spectral trend or other supporting evidence suggests a disturbance or change event has occurred, but the definitive cause cannot be determined, or the type of change fails to meet any of the change process categories defined above.
    10. GROWTH/RECOVERY: Land exhibiting an increase in vegetation cover due to growth and succession over one or more years. Applicable to any areas that may express spectral change associated with vegetation regrowth. In developed areas, growth can result from

maturing vegetation and/or newly installed lawns and landscaping. In forests, growth includes vegetation growth from bare ground, as well as the over topping of intermediate and co-dominate trees and/or lower-lying grasses and shrubs. Growth/recovery segments recorded following forest harvest will likely transition through different land cover classes as the forest regenerates. For these changes to be considered growth/recovery, spectral values should closely adhere to an increasing trend line (e.g., a positive slope that would, if extended to ~20 years, be on the order of .10 units of NDVI) that persists for several years.

- Land cover
    1. TREES: Live or standing dead trees.
    2. TALL SHRUBS (SEAK only): Shrubs > 1 m in height.
    3. SHRUBS: Shrubs.
    4. GRASS/FORB/HERBACEOUS: Perennial grasses, forbs, or other forms of herbaceous vegetation.
    5. BARREN OR IMPERVIOUS: a) Bare soil exposed by disturbance (e.g., soil uncovered by mechanical clearing or forest harvest), as well as perennially barren areas such as deserts, playas, rock outcroppings (including minerals and other geologic materials exposed by surface mining activities), sand dunes, salt flats, and beaches. Roads made of dirt and gravel are also considered barren; or b) man-made materials that water cannot penetrate, such as paved roads, rooftops, and parking lots.
    6. SNOW/ICE: Snow and/or ice.
    7. WATER: Water.
- Land use
    1. AGRICULTURE: Land used to produce food, fiber and fuels which is in either a vegetated or non-vegetated state. This includes but is not limited to cultivated and uncultivated croplands, hay lands, orchards, vineyards, confined livestock operations, and areas planted for production of fruits, nuts or berries. Roads used primarily for agricultural use (i.e., not used for public transport from town to town) are considered agriculture land use.
    2. DEVELOPED: Land covered by man-made structures (e.g., high density residential, commercial, industrial, mining or transportation), or a mixture of both vegetation (including trees) and structures (e.g., low density residential, lawns, recreational facilities, cemeteries, transportation and utility corridors, etc.), including any land functionally altered by human activity.
    3. FOREST: Land that is planted or naturally vegetated and that contains (or is likely to contain) 10% or greater tree cover at some time during a near-term successional sequence. This may include deciduous, evergreen and/or mixed categories of natural forest, forest plantations, and woody wetlands.
    4. NON-FOREST WETLAND: Lands adjacent to or within a visible water table (either permanently or seasonally saturated) dominated by shrubs or persistent emergents. These wetlands may be situated shoreward of lakes, river channels, or estuaries; on river floodplains; in isolated catchments; or on slopes. They may also occur as prairie potholes, drainage ditches and stock ponds in agricultural landscapes and may also appear as islands in the middle of lakes or rivers. Other examples also include marshes, bogs, swamps, quagmires, muskegs, sloughs, fens, and bayous.
    5. OTHER: Lands which are perennially covered with snow and ice, water, salt flats and other undeclared classes. Glaciers and ice sheets or places where snow and ice obscure any other land cover call are included (assumed is the presence of permanent snow and ice). Water includes rivers, streams, canals, ponds, lakes, reservoirs, bays, or oceans. This

assumes permanent water (which can be in some state of flux due to ephemeral changes brought on by climate or anthropogenic).

6. RANGELAND/PASTURE: This class includes any area that is either a) rangeland, where vegetation is a mix of native grasses, shrubs, forbs and grass-like plants largely arising from natural factors and processes such as rainfall, temperature, elevation and fire, although limited management may include prescribed burning as well as grazing by domestic and wild herbivores; or b) pasture, where vegetation may range from mixed, largely natural grasses, forbs and herbs to more managed vegetation dominated by grass species that have been seeded and managed to maintain near monoculture.

Calibration Data Finalization

Since the classes listed above can be too detailed to model with remote sensing data, we bin (cross-walk) them into larger classes appropriate for the LCMS modeling methods. Change processes are cross-walked into three final classes:

- Slow Loss
  - Structural decline
  - Spectral decline
- Fast Loss
  - Fire
  - Harvest
  - Mechanical
  - Wind/ice
  - Hydrology
  - Debris
  - Other
- Gain
  - Growth/recovery

Land cover requires a different cross-walking approach. All TimeSync plots have a primary land cover class that makes up the majority of the plot. Any additional land cover class that comprises 10% or more of the plot is assigned as a secondary land cover class. Since a plot may have any number of secondary land cover classes, primary/secondary combinations of interest are modeled separately. We include any primary/secondary combination that is common along typical succession, focusing on pairings with a secondary class that is higher along the successional order. The expected land cover successional order is: barren to grass/forb/herb, grass/forb/herb to shrub, and shrub to tree. With this in in mind, the primary/secondary land cover combinations we model in LCMS are shown in Table 5.

Table 5. – List of primary and secondary land cover classes modeled in LCMS. Successional classes are grouped and highlighted with italic font. The snow/ice and water classes are not modeled with any secondary land cover classes since they are not likely to be part of vegetation succession.

Primary	Secondary
Trees	NA
Tall Shrubs	*Trees*
Shrubs	*Trees*
Grass/forb/herb	*Trees*
Barren	*Trees*
Tall Shrubs	NA
Shrubs	NA
Grass/forb/herb	*Shrubs*
Barren	*Shrubs*
Grass/forb/herb	NA
Barren	*Grass/forb/herb*
Barren or Impervious	NA

We take the land use classes directly from the TimeSync plots:

- Agriculture
- Developed
- Forest
- Non-forest wetland
- Other
- Rangeland or pasture

Model predictor data

We use spectral information from Landsat and Sentinel-2 imagery and topographic information from the USGS 3D Elevation Program (3DEP) for modeling. Descriptions of each of these datasets are provided below.

Remote sensing spectral data

Data preparation

LCMS uses United States Geological Survey (USGS) Collection 2 Tier 1 Landsat 4, 5, 7, 8 and 9 and Sentinel-2a and -2b level 1C top of atmosphere reflectance data. We do not use surface reflectance data because the Sentinel-2 surface reflectance data available within GEE are terrain-corrected. This makes it difficult to utilize in unison with Landsat surface reflectance data that are not terrain-corrected.

The exception was CCDC data for the CONUS that used surface reflectance data. While v2022.8 CONUS utilized surface reflectance data for CCDC, it was later discovered that the surface reflectance correction algorithm does not work well over snow, ice, and water (U.S. Geological Survey, 2023). Reflectance values frequently are less than 0 or greater than 1. For this reason, CCDC in other study areas will use top of atmosphere reflectance data. CONUS will likely adopt this practice in future versions.

For cloud masking Landsat data, we apply the CFmask cloud masking algorithm (Foga et al., 2017), which is an implementation of Fmask 2.0 (Zhu and Woodcock 2012), as well as the cloudScore algorithm (Chastain et al., 2019). For cloud masking Sentinel-2 data, we utilize the s2Cloudless algorithm. We mask

cloud shadows in both Landsat and Sentinel-2 using the Temporal Dark Outlier Mask (TDOM) method (Chastain et al., 2019). All remote sensing data preparation procedures can be accessed in the GTAC GEE data processing and visualization library (GTAC GEE Visualization Python Modules on PyPI, GTAC GEE Visualization Python Modules on GitHub).

Annual compositing

LCMS utilizes cloud/cloud shadow masked data as well as annual composites of these data to meet the needs of the temporal segmentation methods. Annual composite values are the geometric medoid of all values not masked as cloud or cloud shadow from a specified date range for each year. Due to differences in data availability and seasonality, we vary the date range across different modeling regions and time (Table 6).

Table 6. – Dates used for annual compositing of Landsat and Sentinel-2 data.

Study Area	Pre Sentinel-2 Start Date	Pre Sentinel-2 End Date	Post Sentinel-2 Start Date	Post Sentinel-2 End Date
CONUS	June 1	September 30	July 1	September 1
SEAK	June 15	September 15	June 15	September 15
PRUSVI	June 1	May 31	June 1	May 31
HA	January 1	December 31	January 1	December 31

The geometric medoid is the value that minimizes the sum of the square difference between the median value of each band's values. This ensures that the center-most value in a multi-dimensional feature space is chosen. The value from all bands is from the same observation date. The bands that we include in the feature space are green, red, near infrared (NIR), first shortwave infrared (SWIR1), and second shortwave infrared (SWIR2). We omit blue because it is more prone to atmospheric scattering and can inappropriately influence the medoid algorithm. Any pixel that does not have a cloud or cloud shadow free value for a given year is left as null and excluded from any map for that year. The 2020 composite images for CONUS and SEAK are shown in Figure 6 as an example.

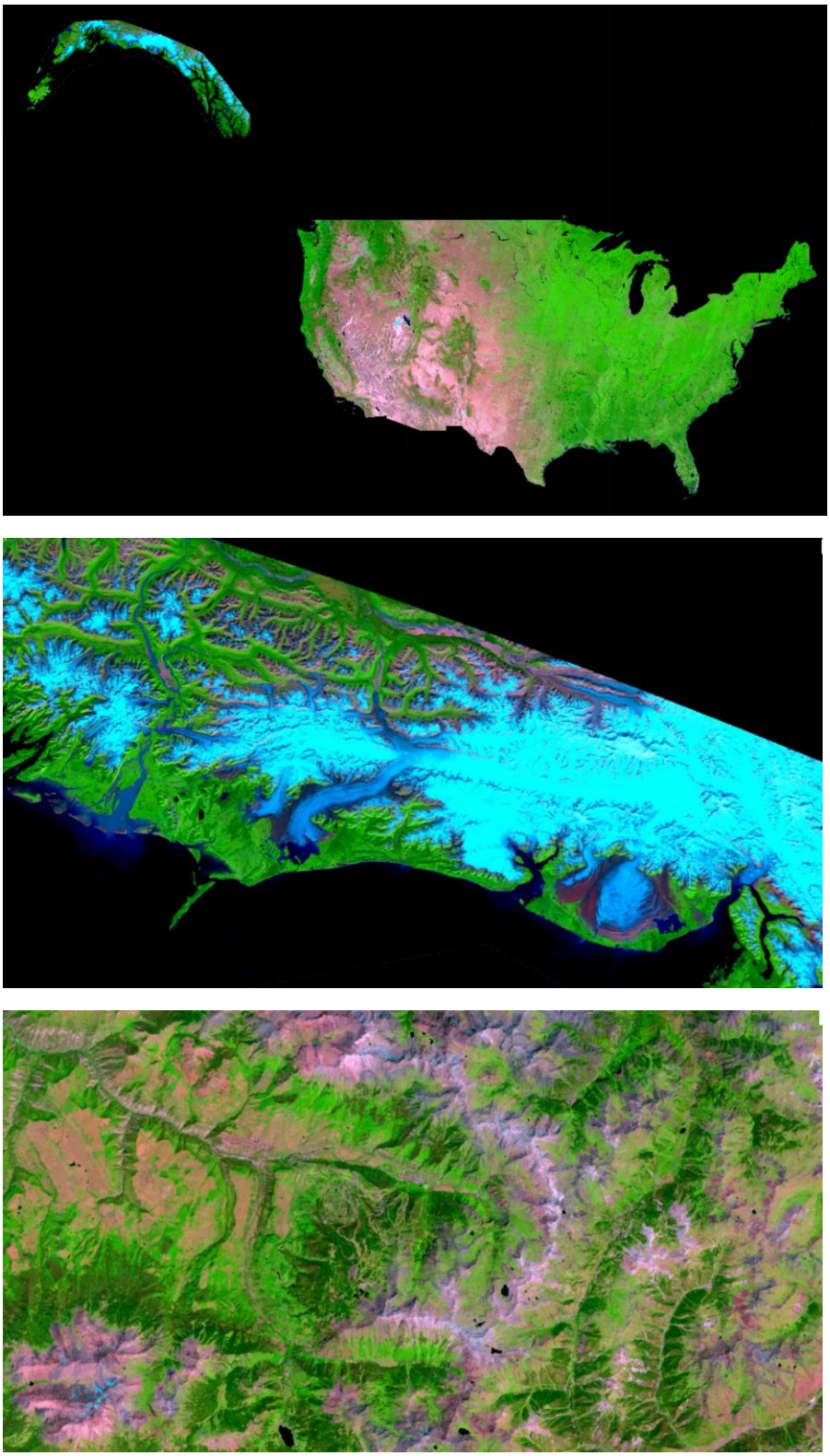

Figure 6. – Example of the 2020 composites used in the Land Change Monitoring System (LCMS). The red, green, and blue channels used in these composites are the second shortwave infrared (SWIR2), near infrared (NIR), and red bands, respectively. The top image shows both southeast Alaska (SEAK) and the conterminous United States (CONUS). The middle image shows a portion of coastal AK, while the bottom image shows a zoomed in view over Telluride, CO.

Temporal segmentation

The goal of temporal segmentation is to identify periods of time that likely have similar land cover and/or change processes. Since different segmentation methods have advantages and disadvantages, LCMS utilizes the ensemble approach outlined in Cohen et al., (2018) and Healey et al., (2018). Currently, the operational version of LCMS utilizes LandTrendr (Kennedy et al., 2010; Kennedy et al., 2018) and CCDC (Zhu and Woodcock 2014) to segment the prepared time series. LandTrendr requires a maximum of one observation per year (i.e., an annual composite, made from Landsat and Sentinel-2 data), while CCDC utilizes every available cloud and cloud shadow-free observation from the Landsat time series only.

LandTrendr Methods

LandTrendr iteratively breaks the time series of annual composites and returns a set of segments. Each segment has a start and end year and a start and end fitted value at the start and end vertices respectively (Figure 7).

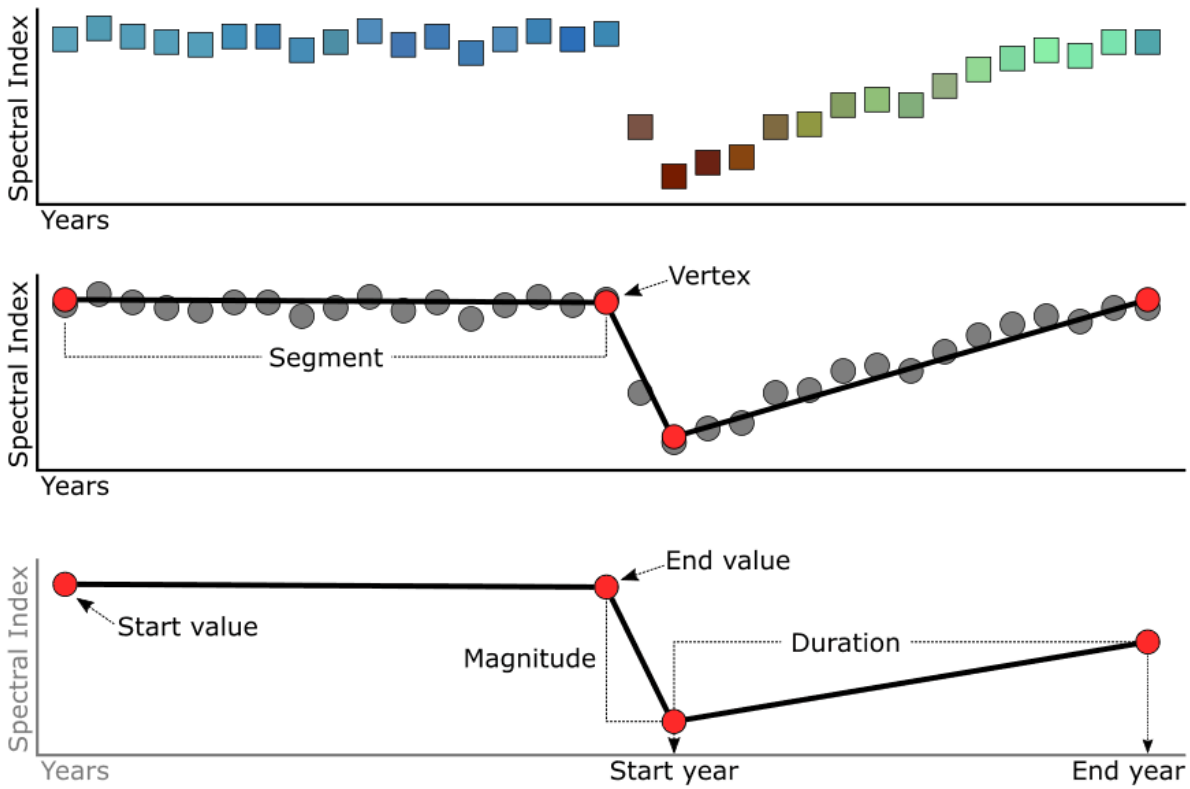

Figure 7. – Illustration from https://emapr.github.io/LT-GEE/ depicting how LandTrendr breaks a time series and the information that can be taken from the output.

From this information, we assign each band/index for each year the following values:

- Fitted value
- Difference of that year's fitted value from the fitted value of the start vertex
- Difference from the start to end fitted value of the segment that year falls in
- The duration of the segment that year falls in
- The slope of the segment that year falls in

LCMS uses the GEE version of LandTrendr outlined in Kennedy et al., (2018). The parameters that are used are the same as those in Kennedy et al., (2018) (Table 7).

Table 7. – LandTrendr parameters used

Parameter Name	Value	Description
maxSegments	6	Maximum number of segments to be fitted on the time series.
spikeThreshold	0.9	Threshold for damping the spikes (1.0 means no dampening).
vertexCountOvershoot	3	The initial model can overshoot the maxSegments + 1 vertices by this amount. Later, it will be pruned down to maxSegments + 1.
preventOneYearRecovery	true	Prevent segments that represent one-year recoveries.
recoveryThreshold	0.25	If a segment has a recovery rate faster than 1/recoveryThreshold (in years), then the segment is disallowed.
pvalThreshold	0.05	If the p-value of the fitted model exceeds this threshold, then the current model is discarded and another one is fitted using the Levenberg-Marquardt optimizer.
bestModelProportion	1.25	Takes the model with most vertices that has a p-value that is at most this proportion away from the model with lowest p-value.

Further documentation of the LandTrendr method used can be found in the GEE reference documentation.

CCDC Methods

CCDC segments the time series by identifying outliers from a harmonic regression model. The idea is that different land cover and/or land use types have distinct seasonality signatures. A departure from the seasonality signature indicates a change (Figure 8).

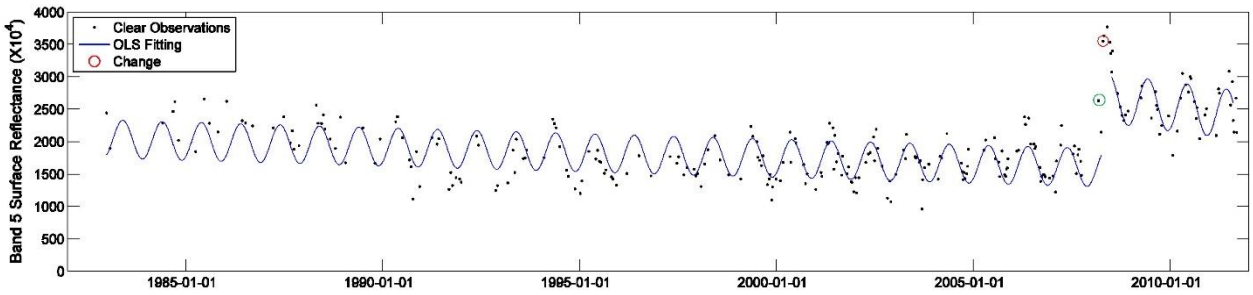

Figure 8. – An example of how Continuous Change Detection and Classification (CCDC) segments a time series of data. The clear observations for band 5 (first shortwave infrared band for Land Change Monitoring System [LCMS]) are shown as dots, while the modeled value is shown as a blue line. Notice the dots depart from the typical values around 2008. CCDC then starts a new model following this departure when a new consistent seasonal pattern is re-established. (Source: Zhu and Woodcock 2014 figure 21)

Input data include all Landsat cloud and cloud shadow-free values. LCMS uses all cosine and sine coefficients from the first three harmonics (2π, 4π, and 6π; see Zhu and Woodcock 2014) from the CCDC outputs. We do not use the slope and intercept generated by CCDC. Instead, we use the predicted value based on the harmonic model on September 1 in place of the intercept (Figure), and the difference between that year and the previous year's fitted values as the slope. This allows CCDC to work properly within the LCMS annual ensemble framework.

The GEE version of CCDC is used for LCMS. The parameters used are shown in Table 8.

Table 8. Continuous Change Detection and Classification (CCDC) parameters used.

Parameter Name	Value	Description
breakpointBands	["green","red","nir","swir1", "swir2"]	The name or index of the bands to use for change detection. If unspecified, all bands are used.
tmaskBands	null	The name or index of the bands to use for iterative TMask cloud detection. These are typically the green band and the SWIR2 band. If unspecified, TMask is not used. If specified, 'tmaskBands' must be included in 'breakpointBands'.
minObservations	6	The number of observations required to flag a change.
chiSquareProbability	0.99	The chi-square probability threshold for change detection in the range of [0, 1]
minNumOfYearsScaler	1.33	Factors of minimum number of years to apply new fitting.
dateFormat	1	The time representation to use during fitting: 0 = jDays, 1 = fractional years, 2 = unix time in milliseconds. The start, end and break times for each temporal segment will be encoded this way.
lambda	0.002	Lambda for LASSO regression fitting. If set to 0, regular OLS is used instead of LASSO.
maxIterations	25000	Maximum number of runs for LASSO regression convergence. If set to 0, regular OLS is used instead of LASSO.

Further documentation of the CCDC methods used can be found in the GEE reference documentation.

Summary
Visualizing how the medoid composites and fitted LandTrendr and CCDC values relate can be quite difficult. Figure 9 attempts to illustrate how these values relate for two example pixels. The pixel depicted in the left column shows a fire event, while the right column shows insect-related tree mortality.

The first row shows the time series of the medoid composite values. Notice how each band relates to the other during the change events. The middle row shows the normalized burn ratio (NBR) (a vegetation index related to moisture levels) fitted CCDC output, along with the annualized CCDC value from September 1 for each year. Notice how CCDC finds a break for the fire example but shows a single long-term declining trend of NBR for the insect-related mortality. The bottom row shows the annual values of NBR from the medoid composites, LandTrendr, and CCDC. This illustrates how all three directly relate to each other. Each is different, but not necessarily right or wrong. Both LandTrendr and CCDC reduce inter-annual noise but identify breaks at different points in time. These are all used in the random forest model outlined below to produce final LCMS products.

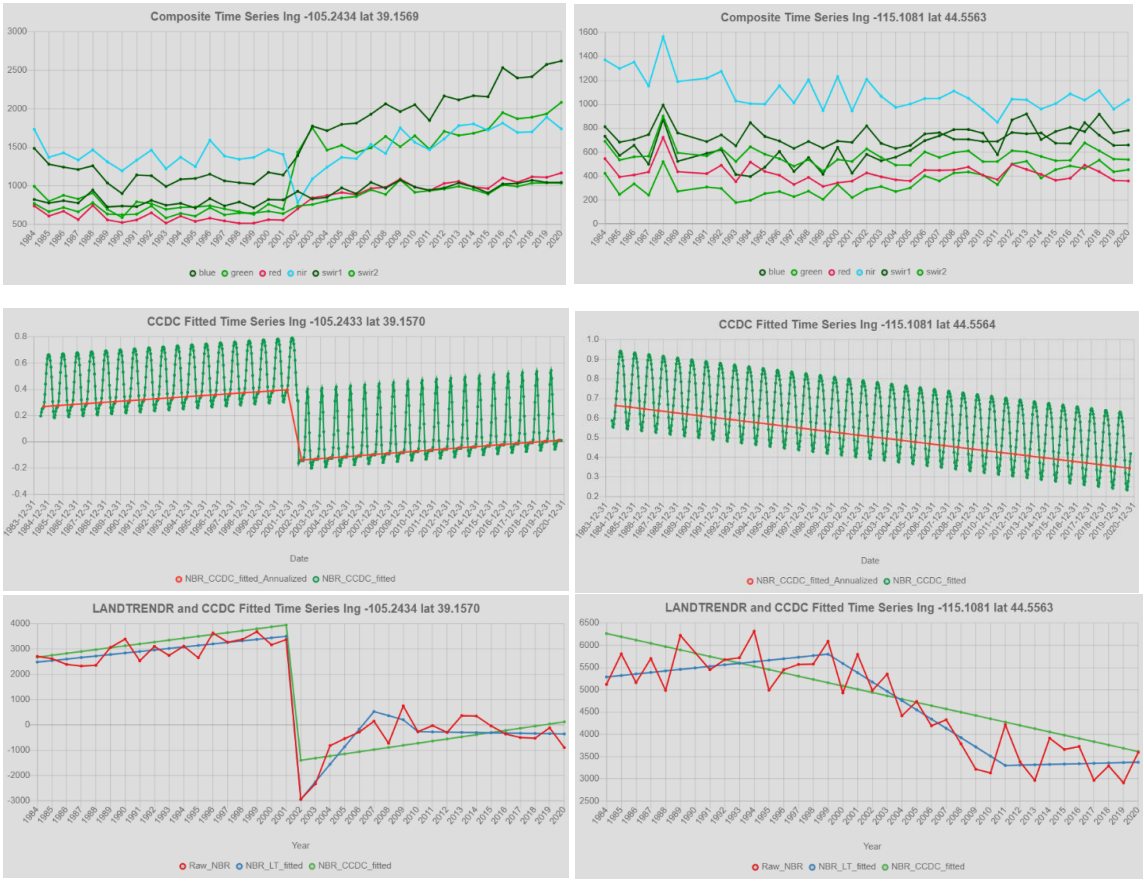

Figure 9. – An example of predicted values from a pixel. The left column depicts a pixel with a fire event, while the right column depicts a pixel with insect-related tree mortality. The top row shows the raw spectral bands from the annual medoid composites. The second row shows the Continuous Change Detection and Classification (CCDC) output for the normalized burn ratio (NBR) vegetation index, as well as the annualized values used in the Land Change Monitoring System (LCMS). The bottom row shows the raw NBR, LandTrendr-fitted NBR, and CCDC-fitted NBR values on a single graph. This illustrates how these data complement each other as well as how they differ.

Terrain data

LCMS also uses terrain metrics to provide elevation, slope, aspect, and slope-position information to the model. The specific variables used are:

- Elevation
- Sine (Aspect)
- Cosine (Aspect)
- Slope
- Slope-position (circular kernel with 11 pixel window, 21 pixel window, and 41 pixel window) (Weiss 2001)

For all study areas the 10 m USGS 3D Elevation Program (3DEP) data was used (U.S. Geological Survey, 2019). All resampling was performed using cubic convolution.

Summary

All variables covered in this section are utilized in the methods outlined below. Table 9 shows a full list of all predictor variables considered for modeling. Not included in this list is Landsat thermal data that is used as a predictor variable in 2022.8 CONUS modeling.

			LANDTRENDR (Landsat and Sentinel 2)					CCDC (Landsat only)								Terrain
			LANDTRENDR Fitted	LANDTRENDR Diff	LANDTRENDR Dur	LANDTRENDR Mag	LANDTRENDR Slope	CCDC Fitted	CCDC Fitted Slope	CCDC COS 1	CCDC COS 2	CCDC COS 3	CCDC SIN 1	CCDC SIN 2	CCDC SIN 3	Raw
Annual	Spectral Bands	blue	✓	✓	✓	✓	✓	✓	✓	✓	✓	✓	✓	✓	✓	
		green	✓	✓	✓	✓	✓	✓	✓	✓	✓	✓	✓	✓	✓	
		red	✓	✓	✓	✓	✓	✓	✓	✓	✓	✓	✓	✓	✓	
		nir	✓	✓	✓	✓	✓	✓	✓	✓	✓	✓	✓	✓	✓	
		swir1	✓	✓	✓	✓	✓	✓	✓	✓	✓	✓	✓	✓	✓	
		swir2	✓	✓	✓	✓	✓	✓	✓	✓	✓	✓	✓	✓	✓	
	Indices	NDVI	✓	✓	✓	✓	✓	✓	✓	✓	✓	✓	✓	✓	✓	
		NBR	✓	✓	✓	✓	✓									
		NDMI	✓	✓	✓	✓	✓									
		NDSI	✓	✓	✓	✓	✓									
	Tasseled Cap Transformation	brightness	✓	✓	✓	✓	✓									
		greenness	✓	✓	✓	✓	✓									
		wetness	✓	✓	✓	✓	✓									
		brightness / greenness angle	✓	✓	✓	✓	✓									
Single Value	Terrain	Elevation														✓
		Slope														✓
		cos(Aspect)														✓
		sin(Aspect)														✓
		TPI (11 pixel)														✓
		TPI (21 pixel)														✓
		TPI (41 pixel)														✓

Table 9. – List of Land Change Monitoring System (LCMS) model predictor variables. Annual values are different for each year of the analysis period, while the single value terrain variables remain constant.

Modeling (Supervised Classifications)

All supervised classifications for LCMS utilize the random forest modeling method (Breiman 2001). Random forest randomly selects a subset of the predictor variables and training sites in many different classification and regression trees. Each of the many trees predicts a class, which are then aggregated and used to determine the final modeled class.

LCMS utilizes the GEE instance of random forests called “smileRandomForest” for all raster-based classification. Local processing utilized for variable selection and map validation uses the sklearn.ensemble.RandomForestClassifier method.

LCMS uses a separate random forest model for each of the following products:

- Change (3 separate single class models)
    - Slow Loss

    - Fast Loss
    - Gain
- Land cover (1 multi-class model)
- Land use (1 multi-class model)

Each of these products has an annual model output that is the proportion of trees within the random forest model that chose each class. Each change class has a separate model, while land cover and land use each have a single model with the proportion of trees for more multiple classes. For example, if the fast loss random forest model had a total of 100 classification trees in it, and 45 of those trees chose "fast loss" and 65 chose "not fast loss" in 2005, that pixel would have a value of 0.45 in 2005. This model confidence, which can also be thought of as a probability, can have values between 0 and 1 and is available for each model for each year from 1985 to the most recent complete growing season. Figure 10 illustrates this concept in more detail.

Predictor variable selection

To reduce predictor variable co-variation and inclusion of variables that do not improve the model, we filter predictor variables in a two-step process. The first step involves filtering out any predictor pairs that have an r-squared greater than 0.95 (pandas.DataFrame.corr). The variable with the lowest mean r-squared across all pairs is retained. The next step is a recursive feature elimination using a 5-fold grouped cross validation (sklearn.feature_selection.RFECV). We retain the variable combination with the highest accuracy for land use and land cover or highest ROC_AUC (Area Under the Receiver Operating Characteristic Curve) score for change.

Model validation

We determine an optimum model confidence threshold by assessing the precision and recall at every possible threshold (from 0-100) and selecting the threshold that maximizes both precision and recall. We then use this threshold in a stratified 5-fold cross validation following Stehman (2014) for each change, land cover, and land use model. We use the stratified random sample of 30 m by 30 m plot locations as the sample, and group training points by plot ID so that all training points from the same plot (but that occurred in different years) are always included in the same fold.

Final output creation

As explained above, each class within the change, land cover, and land use products has a model confidence score, which represents the proportion of trees within the random forest model that classified a given pixel as that class for that model. Some examples of model confidence time series from individual pixels are shown in Figure 10. For each year, the line with the highest confidence is the class that is chosen for the given LCMS product (change, land cover, and land use). For change classes, the line with the highest confidence must also have a value above that model's threshold. This is done because the "Stable" class is not modeled explicitly.

In Figure 10, the pixel time series shown in the left column has been affected by a fire, while the pixel shown in the right column depicts long-term tree mortality from insects. The first, second, and third rows show the change, land cover, and land use time series, respectively.

Beginning with the fire example, the change time series (first row, left column) shows that the *fast loss* model confidence peaks in the year of the fire (2012), to a value that exceeds the fast loss threshold of 0.29. In the years following the fire (2013-2020), the *gain* model confidence rises to levels above the gain threshold of 0.29, as one might expect with growth and recovery following a fire. Complementing the change time series, the land cover time series (second row, left column) shows that the *tree* class had a

very high model confidence for each year until the fire in 2012. Following the fire, the *tree* model confidence goes down, but it remains the most confident class. This often occurs when the trees are damaged or not all burned, but the understory burns. In the following years, we see the probability of *grass/forb/herb & trees mix* increase, most likely indicating that there are live trees in this pixel with grasses becoming more and more prevalent. Since a fire generally does not indicate a land use transition, the land use *forest* model's confidence dips (third row, left column), but remains the highest.

The time series of long-term tree mortality caused by beetles (right column), is quite different. In this case, the *slow loss* model confidence is elevated for about two decades (first row, right column). While the *gain* model confidence is elevated slightly during the second decade of this trend, the *slow loss* model remains the highest. Although there was indeed slow loss at this pixel, there was no transition of land cover or land use classes (second and third rows, right column). It is important to note that many instances of loss and gain do not result in a change of land cover or land use.

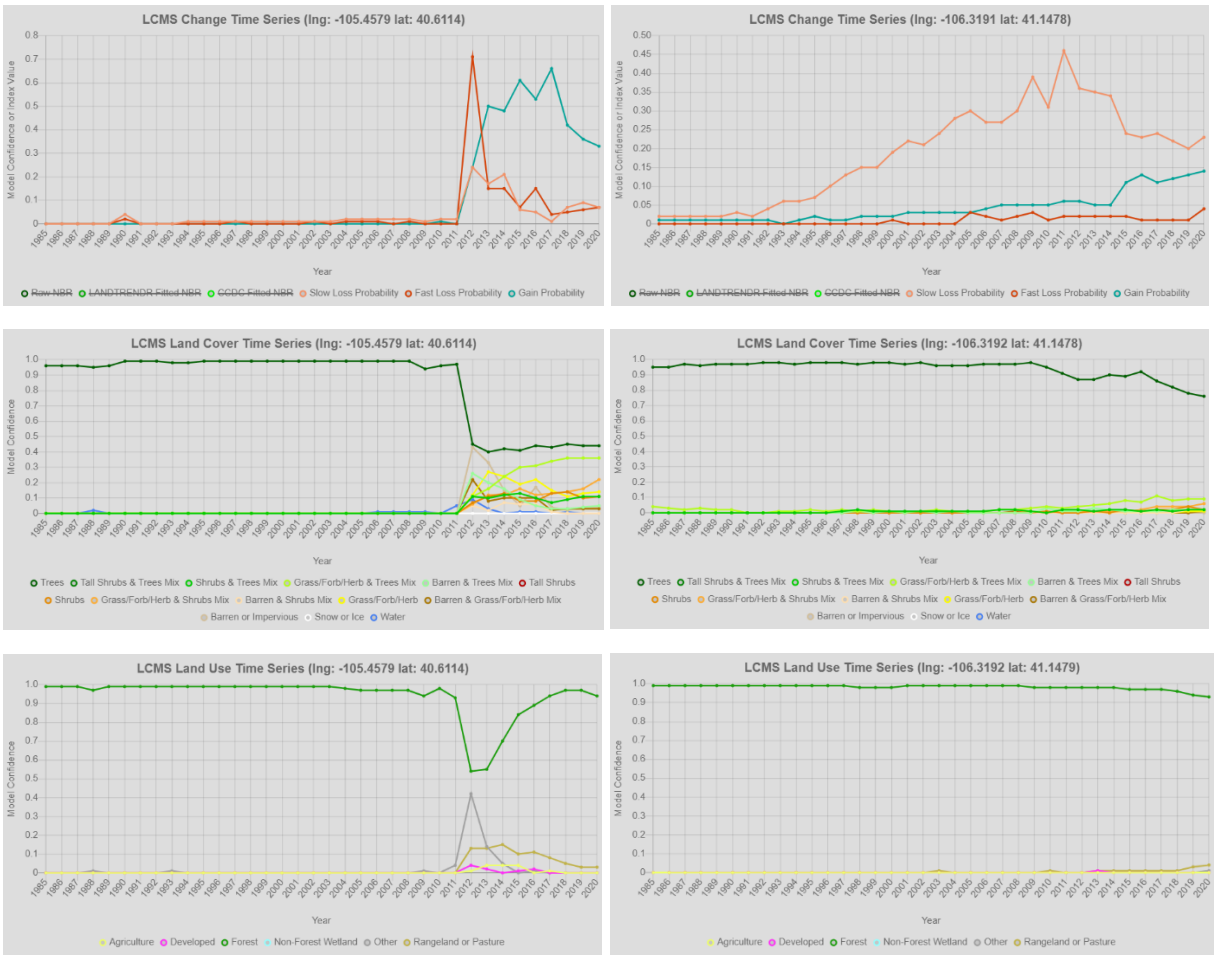

Figure 10. – Time series of Land Change Monitoring System raw modeled probabilities for each year for a fire (left column) and tree mortality due to beetles (right column). The first, second, and third rows of this figure show the change, land cover, and land use time series, respectively. The map product assumes the class with the highest confidence for each year. Notice that it is possible to have a change event without a change in land cover or land use.

LCMS products

We package the final LCMS deliverables in two ways: annual and summarized layers. For each product (change, land cover, and land use) we assemble annual maps, as discussed above. We only provide summary products for change since only change products can easily be summarized. Beyond providing the mode for land cover and land use products, summarizing them is rather difficult.

To summarize the change layers, we use two methods: *most recent* and *most probable*. The *most recent* method chooses the year of the respective change class that occurred most recently, while the *most probable* method chooses the year of the respective change class with the highest model confidence. The former can be useful for applications that need to know the most recent year a given change class was present, while the latter is useful for applications that need to know when a given change event peaked.

For example, the time series of change model confidences, or probabilities, for a given pixel is shown in figure 11.

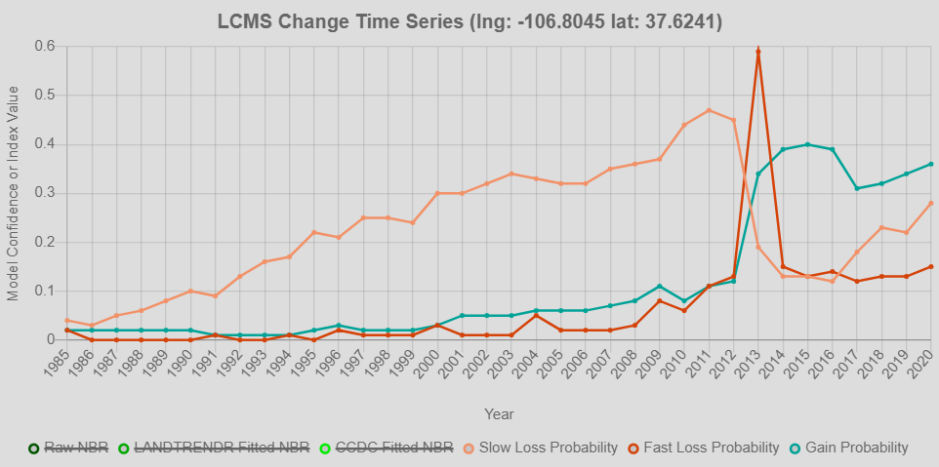

Figure 11. – Land Change Monitoring System change model confidence values for a single pixel.

The *most recent* change years for this example are:

- Slow loss: 2012
- Fast loss: 2013
- Gain: 2020

The *most probable* change years are:

- Slow loss: 2011
- Fast loss: 2013
- Gain: 2015

Generally, the two summary methods differ most for long-term change processes, such as gain and slow loss.

Ancillary information on the origin of the annual LCMS product output values is now provided as part of a QA bit layer. This layer includes whether an interpolated value was used to produce the LCMS output, the sensor, and the day of year the value came from. The QA bits are as follows:

- 1: Interpolated (0), not interpolated (1)
- 2-6: Which sensor the pixel came from
    - 4 = Landsat 4
    - 5 = Landsat 5
    - 7 = Landsat 7
    - 8 = Landsat 8
    - 9 = Landsat 9
    - 21 = Sentinel 2a
    - 22 = Sentinel 2b
- 7-15: Which Julian day the pixel came from (1-365)

Bitwise operations can be leveraged to unpack the QA decimal numbers to valid pixel values for the non-interpolated data, sensor, and Julian day (see metadata for more detailed method). Table 10 shows how the bits are used in the QA Bits output image.

Table 10. – Table of how bits are used in the QA Bits output image.

LCMS QA Band Bits; Read from RIGHT to LEFT, starting with bit 1																
Bit	16	15	14	13	12	11	10	9	8	7	6	5	4	3	2	1
Description		Julian Day									Sensor					Interpolated/Non-interpolated

Useful Resources

- LCMS Website
- LCMS Homepage
- Pilot Product Description
- LCMS Data Explorer
- LCMS Data Downloader
- ESRI Image Services
- LCMS GEE Collection
- LCMS Contact Information

References

Breiman, L. (2001). Random Forests. In Machine Learning (Vol. 45, pp. 5-32). https://doi.org/10.1023/A:1010933404324

Chastain, R., Housman, I., Goldstein, J., Finco, M., & Tenneson, K. (2019). Empirical cross sensor comparison of Sentinel-2A and 2B MSI, Landsat-8 OLI, and Landsat-7 ETM top of atmosphere spectral characteristics over the conterminous United States. In Remote Sensing of Environment (Vol. 221, pp. 274–285). https://doi.org/10.1016/j.rse.2018.11.012

Cohen, W. B., Yang, Z., Healey, S. P., Kennedy, R. E., & Gorelick, N. (2018). A LandTrendr multispectral ensemble for forest disturbance detection. In Remote Sensing of Environment (Vol. 205, pp. 131–140). https://doi.org/10.1016/j.rse.2017.11.015

Cohen, W. B., Yang, Z., & Kennedy, R. (2010). Detecting trends in forest disturbance and recovery using yearly Landsat time series: 2. TimeSync — Tools for calibration and validation. In Remote Sensing of Environment (Vol. 114, Issue 12, pp. 2911–2924). https://doi.org/10.1016/j.rse.2010.07.010

Corbane, C., Florczyk, A., Pesaresi, M., Politis, P., & Syrris, V. (2018). *GHS built-up grid, derived from Landsat, multitemporal (1975-1990-2000-2014), R2018A.* European Commission, Joint Research Centre (JRC). https://doi.org/doi:10.2905/jrc-ghsl-10007

Foga, S., Scaramuzza, P.L., Guo, S., Zhu, Z., Dilley, R.D., Beckmann, T., Schmidt, G.L., Dwyer, J.L., Hughes, M.J., Laue, B. (2017). Cloud detection algorithm comparison and validation for operational Landsat data products. In Remote Sensing of Environment (Vol. 194, pp. 379-390). http://doi.org/10.1016/j.rse.2017.03.026.

Gorelick, N., Hancher, M., Dixon, M., Ilyushchenko, S., Thau, D., & Moore, R. (2017). Google Earth Engine: Planetary-scale geospatial analysis for everyone. In Remote Sensing of Environment (Vol. 202, pp. 18–27). https://doi.org/10.1016/j.rse.2017.06.031

Healey, S. P., Cohen, W. B., Yang, Z., Kenneth Brewer, C., Brooks, E. B., Gorelick, N., Hernandez, A. J., Huang, C., Joseph Hughes, M., Kennedy, R. E., Loveland, T. R., Moisen, G. G., Schroeder, T. A., Stehman, S. V., Vogelmann, J. E., Woodcock, C. E., Yang, L., & Zhu, Z. (2018). Mapping forest change using stacked generalization: An ensemble approach. In Remote Sensing of Environment (Vol. 204, pp. 717–728). https://doi.org/10.1016/j.rse.2017.09.029

Helmer, E. H., Ramos, O., del MLópez, T., Quiñónez, M., & Diaz, W. (2002). Mapping the forest type and land cover of Puerto Rico, a component of the Caribbean biodiversity hotspot. *Caribbean Journal of Science*, (Vol. 38, Issue ¾, pp. 165-183)

Kennedy, R. E., Yang, Z., & Cohen, W. B. (2010). Detecting trends in forest disturbance and recovery using yearly Landsat time series: 1. LandTrendr — Temporal segmentation algorithms. In Remote Sensing of Environment (Vol. 114, Issue 12, pp. 2897–2910). https://doi.org/10.1016/j.rse.2010.07.008

Kennedy, R., Yang, Z., Gorelick, N., Braaten, J., Cavalcante, L., Cohen, W., & Healey, S. (2018). Implementation of the LandTrendr Algorithm on Google Earth Engine. In Remote Sensing (Vol. 10, Issue 5, p. 691). https://doi.org/10.3390/rs10050691

Olofsson, P., Foody, G. M., Herold, M., Stehman, S. V., Woodcock, C. E., & Wulder, M. A. (2014). Good practices for estimating area and assessing accuracy of land change. In Remote Sensing of Environment (Vol. 148, pp. 42–57). https://doi.org/10.1016/j.rse.2014.02.015

Pedregosa, F., Varoquaux, G., Gramfort, A., Michel, V., Thirion, B., Grisel, O., Blondel, M., Prettenhofer, P., Weiss, R., Dubourg, V., Vanderplas, J., Passos, A., Cournapeau, D., Brucher, M., Perrot, M. and Duchesnay, E. (2011). Scikit-learn: Machine Learning in Python. In Journal of Machine Learning Research (Vol. 12, pp. 2825-2830).

Pengra, B. W., Stehman, S. V., Horton, J. A., Dockter, D. J., Schroeder, T. A., Yang, Z., Cohen, W. B., Healey, S. P., & Loveland, T. R. (2020). Quality control and assessment of interpreter consistency of

annual land cover reference data in an operational national monitoring program. In Remote Sensing of Environment (Vol. 238, p. 111261). https://doi.org/10.1016/j.rse.2019.111261

Sentinel-Hub (2021). Sentinel 2 Cloud Detector. [Online]. Available at: https://github.com/sentinel-hub/sentinel2-cloud-detector (Accessed: 2021)

Stehman, S.V. (2014). Estimating area and map accuracy for stratified random sampling when the strata are different from the map classes. In International Journal of Remote Sensing (Vol. 35, pp. 4923-4939). https://doi.org/10.1080/01431161.2014.930207

U.S. Geological Survey, 2019, USGS 3D Elevation Program Digital Elevation Model, accessed August 2022 at https://developers.google.com/earth-engine/datasets/catalog/USGS_3DEP_10m

U.S. Geological Survey, 2023, Landsat Collection 2 Known Issues, accessed March 2023 at **https://www.usgs.gov/landsat-missions/landsat-collection-2-known-issues**

Weiss, A.D. (2001). Topographic position and landforms analysis Poster Presentation, ESRI Users Conference, San Diego, CA

Yang, L., Jin, S., Danielson, P., Homer, C., Gass, L., Case, A., Costello, C., Dewitz, J., Fry, J., Funk, M., Grannemann, B., Rigge, M., and Xian, G. (2018). A New Generation of the United States National Land Cover Database: Requirements, Research Priorities, Design, and Implementation Strategies (https://www.sciencedirect.com/science/article/abs/pii/S092427161830251X), (pp. 108–123)

Zhu, Z., & Woodcock, C. E. (2012). Object-based cloud and cloud shadow detection in Landsat imagery. In Remote Sensing of Environment (Vol. 118, pp. 83–94). https://doi.org/10.1016/j.rse.2011.10.028

Zhu, Z., & Woodcock, C. E. (2014). Continuous change detection and classification of land cover using all available Landsat data. In Remote Sensing of Environment (Vol. 144, pp. 152–171). https://doi.org/10.1016/j.rse.2014.01.011